

Cortical oscillatory dysrhythmias in visual snow syndrome: a magnetoencephalography study

*Dr Jenny L. Hepschke MBBS, BSc(Med) MD^{1,2}, *Dr. Robert A Seymour PhD^{3,5}, Dr. Wei He PhD³, Dr. Andrew Etchell PhD³, Associate Professor Paul F Sowman PhD³, Associate Professor Clare L Fraser MBBS MMed FRANZCO^{1,4}

**Joint first authors*

1. Save Sight Institute, Faculty of Health and Medicine, The University of Sydney, Sydney, NSW Australia
2. Department of Ophthalmology, Prince of Wales Hospital, High Street, Randwick, NSW, Australia
3. Department of Cognitive Science, Macquarie University, Sydney NSW Australia
4. Macquarie Ophthalmology, Macquarie University, Sydney NSW, Australia
5. Wellcome Centre for Human Neuroimaging, UCL Queen Square Institute of Neurology, University College London, London WC1N 3AR, United Kingdom.

Correspondence to:

Dr Clare L Fraser, Save Sight Institute, 8 Macquarie Street, Sydney, NSW Australia.

Phone: +61 2 9382 7300. Email: clare.fraser@sydney.edu.au

Short title (Running head): Dysrhythmias in Visual Snow Syndrome

1 **Abstract:**

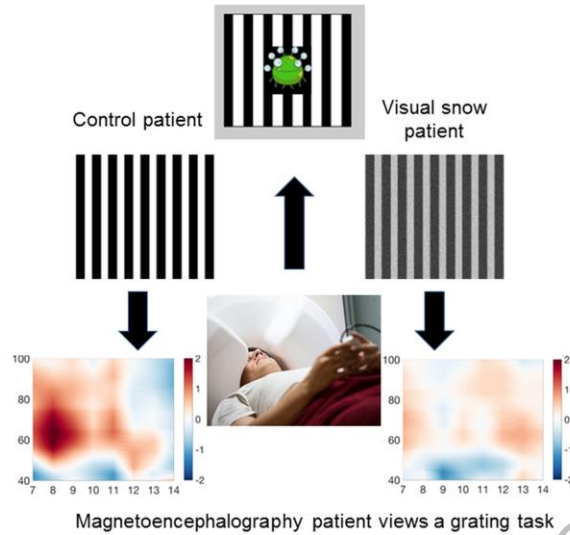
2 Visual Snow refers to the persistent visual experience of static in the whole visual field of both eyes. It is
3 often reported by patients with migraine and co-occurs with conditions like tinnitus and tremor. The
4 underlying pathophysiology of the condition is poorly understood. Previously we hypothesised, that
5 visual snow syndrome may be characterised by disruptions to rhythmical activity within the visual
6 system.

7 To test this, data from 18 patients diagnosed with visual snow syndrome, and 16 matched controls, were
8 acquired using magnetoencephalography. Participants were presented with visual grating stimuli, known
9 to elicit decreases in alpha-band (8-13Hz) power and increases in gamma-band power (40-70Hz).

10 Data were mapped to source-space using a beamformer. Across both groups, decreased alpha power and
11 increased gamma power localised to early visual cortex. Data from the primary visual cortex were
12 compared between groups. No differences were found in either alpha or gamma peak frequency or the
13 magnitude of alpha power, $p > 0.05$. However, compared with controls, our visual snow syndrome cohort
14 displayed significantly increased primary visual cortex gamma power, $p = 0.035$. This new electromagnetic
15 finding concurs with previous functional MRI and PET findings suggesting that in visual snow syndrome,
16 the visual cortex is hyper-excitable. The coupling of alpha-phase to gamma amplitude within the primary
17 visual cortex was also quantified. Compared with controls, the visual snow syndrome group had
18 significantly reduced alpha-gamma phase-amplitude coupling, $p < 0.05$, indicating a potential excitation-
19 inhibition imbalance in visual snow syndrome, as well as a potential disruption to top-down “noise-
20 cancellation” mechanisms.

21 Overall, these results suggest that rhythmical brain activity in primary visual cortex is both hyperexcitable
22 and disorganised in visual snow syndrome, consistent with this being a condition of thalamocortical
23 dysrhythmia.

24



1
2
3
4
5
6
7
8
9
10
11
12
13
14
15

Graphical Abstract
159x89 mm (6.2 x DPI)

Keywords:

Visual Snow; Migraine; Dysrhythmia; Magnetoencephalography; Phase Amplitude Coupling

Abbreviations:

- Blood oxygen level dependant (BOLD)
- Decibels (dB)
- Excitatory-inhibitory (E-I)
- Full-field electroretinogram (ffERG)
- Hallucinogen-persistence perceptual disorder (HPPD)
- Iterative closest points (ICP)
- Linearly constrained minimum variance (LCMV)

- 1 Magnetoencephalography (MEG)
- 2 Mean vector length (MVL)
- 3 Montreal Neurological Institute (MNI)
- 4 Pattern electroretinogram (pERG)
- 5 Primary visual cortex (V1)
- 6 Power-amplitude coupling (PAC)
- 7 Region of interest (ROI)
- 8 Standard deviation (SD)
- 9 Visually evoked potential (VEP)
- 10 Visual snow (VS)
- 11 Visual snow syndrome (VSS)
- 12

ACCEPTED MANUSCRIPT

1 Introduction

2 Visual Snow (VS) refers to the persistent visual experience of static in the whole visual field of both eyes,
3 likened to “static analogue television noise”.¹ This phenomena was initially reported by patients with
4 migraine² but more recently has been classified as a syndrome with specific diagnostic criteria to
5 capture the spectrum of the pathology.^{3,4} Visual snow syndrome (VSS) is defined as flickering fine
6 achromatic dots with at least one associated visual symptom of palinopsia², photopsia, nyctalopia, and
7 entoptic phenomena, as well as non-visual symptoms such as tinnitus, migraine, and tremor.^{3,5} Previous
8 epidemiological studies have shown that VSS exists as a continuum and that the frequency of associated
9 non-visual symptoms often carries a higher symptom severity and burden of disease.⁵⁻⁷ The condition
10 has an estimated prevalence of around 2% in the United Kingdom.⁸

11 To date, the pathophysiology underlying VSS is poorly understood, though the high co-prevalence of
12 migraine and tinnitus suggests it may be a disorder of sensory processing.^{1,9} In support of this, recent
13 neuroscientific work has demonstrated various functional and structural alterations within the primary
14 visual cortex (V1),⁵ and ventral visual regions,¹⁰ of VSS patients. Co-occurring hypermetabolism and
15 cortical volume increases at the intersection of right lingual and fusiform gyrus have also recently been
16 reported.⁷ Resting-state functional MRI data from a VSS cohort showed hyperconnectivity between
17 extrastriate and inferior temporal brain regions and prefrontal and parietal regions.¹¹ VSS patients also
18 demonstrate variations in visual evoked potentials,¹² as well as disrupted habituation for repeated
19 stimuli.¹³ Overall, there is an emerging picture of co-occurring visual hyperactivity, hyperconnectivity,
20 and dishabituation in VSS that could result from a faulty “noise-cancelling” mechanism,¹⁴ similar to that
21 in the auditory domain for tinnitus.^{15,16}

22 Our group has recently proposed that VSS symptoms may be underpinned by perturbations to the
23 rhythms of the human visual system,¹: in particular, a disruption to the usual, state-dependent, flow of
24 information within the thalamocortical network. Successful perceptual processing relies upon the
25 coordinated activity of large groups of neuronal cell assemblies throughout the brain, firing in a
26 rhythmic fashion.¹⁷⁻¹⁹ These neuronal “oscillations” can be measured outside the head non-invasively
27 using EEG or magnetoencephalography (MEG).²⁰ We hypothesise that disruptions to visual oscillations
28 may represent a central pathophysiological mechanism in VSS. Specifically, visual dysrhythmia could
29 alter cortical circuit entrainment and top-down control in VSS, thereby altering the threshold for
30 transmission, affecting suppression and attention, and allowing for detection of sub-threshold visual

1 stimuli.^{21,22} Similar disruptions to the endogenous sensory rhythms of the brain are found in other
2 conditions associated with sensory defects, including migraine, neuropathic pain, and tinnitus.²³⁻²⁵

3 This study aimed to investigate the dysrhythmia hypothesis by studying endogenous rhythmical activity
4 (neural oscillations) in the visual system of VSS patients versus controls. We focussed on oscillations in
5 two frequency bands. First, gamma-band (40-100Hz) oscillations; generated locally via the coordinated
6 interaction between excitatory and inhibitory populations of neurons.²⁶ These oscillations are thought to
7 provide a precise timing mechanism,²⁷ to facilitate information transfer up the cortical hierarchy.²⁸
8 Alterations in gamma-band activity have been reported for other conditions of 'phantom' perception,
9 including tinnitus,²⁹⁻³¹ and neuropathic pain.³² Given the reports of hyperexcitability in VSS,⁷ we
10 expected patients to show increased gamma-band power. The second frequency band of interest was
11 the alpha band (8-13Hz). Alpha rhythms are widely observed in EEG and MEG recordings, originating
12 from several cortical and thalamic generators.^{19,33} Alpha power is negatively correlated with sustained
13 attention and is involved in the active inhibition of irrelevant visual information.³⁴ There is emerging
14 evidence that alpha-band oscillations are also involved in long-range functional connectivity,¹⁹ and the
15 modulation of local gamma oscillations within the visual cortex via a phase-amplitude coupling.^{35,36}
16 Given the hypothesised reduction in a top-down, 'noise cancellation' mechanism,^{1,24} we expected VSS
17 patients to show reductions in the modulation of local gamma oscillations via alpha-band phase.

18 We tested these hypotheses using MEG combined with a simple visual-grating paradigm known to elicit
19 reliable changes in both alpha and gamma oscillations in the primary visual cortex.

20 **Materials and Methods**

21 **Participants**

22 Eighteen patients with Visual Snow Syndrome (VSS) and 16 age- and gender-matched controls
23 participated in this study between 2019 and 2020. Before MEG, VS patients underwent a comprehensive
24 examination by a fellowship-trained neuro-ophthalmologist establishing visual snow and migraine
25 diagnosis according to ICD-3 criteria as well as visual and non-visual co-morbidities and previous
26 diagnoses. This included the measurement of visually evoked potential (VEP), pattern electroretinogram
27 (pERG) and full-field electroretinogram (ffERG). VSS participants were included if they fulfilled the
28 diagnostic criteria of typical VS plus at least two additional visual symptoms.³ Participants were excluded
29 if they were taking psychiatric medication, reported epileptic symptoms, had a diagnosis of hallucinogen-

1 persistence perceptual disorder (HPPD), showed any abnormality on brain MRI or visual
2 electrophysiology.

3 **Experimental Procedures**

4 Experimental procedures complied with the Declaration of Helsinki and were approved by Macquarie
5 University Human Research Ethics Committee. Written consent was obtained from all participants.

6 **Experimental Paradigm and Design**

7 Participants performed a visual task (Figure 1) while their brain activity was continuously recorded with
8 MEG. The task contained an embedded black and white visual grating stimulus that has been shown to
9 reliably elicit gamma-band oscillations.^{37,38} Each task trial started with a fixation period (2.0, 3.0, or 4.0s),
10 followed by a monochrome visual grating (spatial frequency of 2 cycles/degree) for 1.5s. Following this,
11 a cartoon picture of an alien or astronaut was presented for 1.0s. This segment of the trial was included
12 only to maintain the engagement and arousal of the participant; the neural response to this stimulus was
13 not analysed. At the end of the trial, participants were presented with a question mark (“?”) and instructed
14 to respond if they had just seen an alien picture using a response pad (maximum response period of 1.0 s).
15 Feedback about the correctness of responses was conveyed to the participant via a short (0.1s) auditory
16 tone. MEG recordings lasted 15-16 minutes and included 150 trials. Accuracy rates were >95% for all
17 participants.

18 **MEG Acquisition**

19 Data were acquired using a KIT MEG160 magnetoencephalograph (Model PQ1160R-N2, KIT,
20 Kanazawa, Japan) consisting of 160 coaxial first-order gradiometers with a 50mm baseline. The KIT
21 MEG160 is arranged in a fixed supine acquisition configuration and is located within a magnetically
22 shielded room (Fujihara Co. Ltd., Tokyo, Japan). Continuous MEG, within a passband of 0.03–200 Hz,
23 was sampled at 1000 Hz. Five head position indicator or “marker” coils were applied for head position
24 measurement, and measurements were taken from these before and after the experiment. No participant
25 moved more than 5mm in any direction (x, y, z) between the two measurements. For MEG-MRI co-
26 registration purposes, three anatomical landmarks (nasion, left pre-auricular, right pre-auricular), the
27 locations of the marker coils, and 1000-5000 points from the head surface were acquired using a
28 Polhemus Fastrak digitizer. A luminance-triggered photodetector output pulse was used to create a
29 temporally precise timestamp upon the presentation of the visual grating.

30 **MEG Preprocessing**

31 Data from two VSS patients and one control participant were contaminated by metal artefacts from non-
32 removable dental implants or jewellery. Temporal signal space separation (0.9 correlation limit) was used

1 to successfully suppress these artefacts in all cases.³⁹ The remaining pre-processing was performed using
2 the Fieldtrip toolbox v20191213.⁴⁰ For each participant, the entire recording was bandpass filtered
3 between 0.5-250Hz (Butterworth filter, 4th order, applied bidirectionally) and band-stop filtered to remove
4 residual 50Hz power-line contamination and its harmonics. Data were then epoched, based on the onset of
5 the visual grating, into segments of 1.5s pre- and 1.5s post-stimulus onset. To avoid edge artefacts during
6 time-frequency decomposition, an additional 2.5s of data on either side of these time-points was included
7 as ‘padding’. MEG channels containing large amounts of artefactual data were identified by visual
8 inspection (a maximum of ten channels, per participant, were removed).

9 Trials containing artefacts (SQUID jumps, eye-blinks, head movement) were removed by visual
10 inspection. After pre-processing, there was an average of 109.7 trials (standard deviation (SD) 9.1) for the
11 VSS group and 117.4 trials for the control group (SD=2.3). Finally, data were down-sampled to 300Hz to
12 speed computation.

13 **MEG-MRI Coregistration**

14 As structural MRI scans were not available for all participants, we adopted an alternative approach for
15 MEG-MRI co-registration. The digitised head-shape data were matched with a database of 95 structural
16 MRIs from the human connectome database,⁴¹ using an iterative closest points (ICP) algorithm. The head
17 shape-MRI pair with the lowest ICP error was then used as a ‘pseudo-MRI’ for subsequent steps. This
18 procedure has been shown to improve source localisation performance in situations where a subject-
19 specific anatomic MRI is not available.^{42,43}

20 The aligned MRI-MEG image was used to create a forward model based on a single-shell description of
21 the inner surface of the skull.⁴⁴ In SPM12, a nonlinear spatial normalisation procedure was used to
22 construct a volumetric grid (8mm resolution) registered to the canonical Montreal Neurological Institute
23 (MNI) brain.

24 **Source-Level Gamma and Alpha Power**

25 Source analysis was conducted using a linearly constrained minimum variance (LCMV) beamformer,⁴⁵
26 which applies a spatial filter to the MEG data at each point of the 8mm grid. Based on recommendations
27 for optimising MEG beamforming,⁴⁶ a regularisation parameter of lambda 5% was used. Beamformer
28 weights were calculated by combining lead-field information with a sensor-level covariance matrix
29 averaged across data from baseline and grating periods. Data were bandpass filtered between 40-70Hz
30 (gamma) and 8-13Hz (alpha), and source analysis was performed separately. To capture induced rather
31 than evoked visual power, a period of 0.3-1.5s following stimulus onset was compared with a 1.2s
32 baseline period (1.5-0.3s before grating onset).

1 **ROI definition**

2 To analyse changes in oscillatory power and power-amplitude coupling (PAC) further, we defined a
3 region of interest (ROI) in the calcarine sulcus using the AAL atlas,⁴⁷ which overlaps with visual area V1.
4 This ROI was chosen based on previous MEG and intracranial recordings,^{28,37,48,49} which has established
5 V1 as the primary cortical generator of gamma oscillations following the presentation of visual grating
6 stimuli. For each participant, we selected the grid-point within the calcarine sulcus (parcel names:
7 *Calcarine_L*; *Calcarine_R*), which showed the greatest change in gamma power versus baseline. The
8 sensor-level data was then multiplied by the spatial filter from this grid-point to obtain a V1 “virtual
9 electrode”.

10 **ROI Oscillatory Power and Peak Frequency**

11 For the gamma band, oscillatory power was calculated using a multi-taper approach,⁵⁰ from 40-70Hz,
12 using a 0.5s time window, sliding in steps of 0.02s and ± 7 Hz frequency smoothing. For the alpha band,
13 oscillatory power was calculated using a single Hanning taper between 8-13Hz, in steps of 1Hz, using a
14 sliding window of 0.1s. The change in oscillatory power between baseline (-1.5 to -0.3s) and visual
15 grating (0.3-1.5s) time-periods was averaged across 40-70Hz (gamma) and 8-13Hz (alpha) and expressed
16 in decibels (dB). This time window was chosen to capture induced rather than evoked visual power. The
17 frequency range 40-70Hz was chosen given previous research showing maximal changes in gamma
18 oscillations for this frequency range.^{28,38,49,50} Post-hoc analysis across a wider frequency range (30-
19 150Hz) confirmed that for our data, both groups showed maximal changes in gamma oscillations
20 between 40-70Hz (see Supplementary Figure 1). To calculate the peak frequency of power changes for
21 each participant, we used MATLAB's *findpeaks.m* function between 40-70Hz (gamma) and 8-13Hz
22 (alpha). Subject-specific results of this procedure are shown in Supplementary Figures 2a-b.

23 **ROI Baseline Power**

24
25 To check whether our results were driven by group differences in baseline power, for each subject, we
26 averaged oscillatory power, as calculated in the previous section, between 1.5s to 0.3s before stimulus
27 onset and 40-70Hz.

28 **V1 Phase-Amplitude Coupling (PAC)**

29 Time courses from our ROI data were examined for changes in alpha-gamma phase-amplitude coupling
30 (PAC). For a detailed discussion about PAC computation and methodological issues, see Seymour,
31 Rippon, & Kessler (2017)³⁸. Briefly, we calculated PAC values between phases 7-13Hz (in 1Hz steps) and

1 amplitudes 34-100Hz (in 2Hz steps) for the time period 0.3-1.5s following the grating presentation. PAC
2 values were corrected using 1.2s of data from the baseline period. This resulted in a 33*7 amplitude-
3 phase comodulogram for VSS and control groups, which were statistically compared using a cluster-
4 based permutation test.⁵¹ A more broadband frequency range for the amplitude was chosen so that we
5 could capture the minimum and maximum edges of increased PAC in the comodulogram. To calculate
6 PAC values, we used the mean vector length (MVL) approach from Ozkurt & Schnitzler⁵². Code used for
7 PAC computation can be found at: <https://github.com/neurofractal/PACmeg>.

8 **Statistical Analysis**

9 V1 oscillatory power and peak frequency were compared between groups using an independent samples t-
10 test (two-tailed) implemented in JASP.⁵³

11 For PAC, statistical analysis was performed using cluster-based permutation tests,⁵¹ which consist of two
12 parts: first, an independent-samples t-test (two-tailed) is performed, and values exceeding an uncorrected
13 5% significance threshold are grouped into clusters. The maximum t-value within each cluster is carried
14 forward. Second, a null distribution is obtained by randomising the participant label (VSS/control) 10,000
15 times and calculating the largest cluster-level t-value for each permutation. The maximum t-value within
16 each original cluster is then compared against this distribution. The null hypothesis is rejected if the test
17 statistic exceeds a threshold of $p < 0.05$ (corrected across both tails, i.e., $p < 0.025$ for each tail).

18 **Data availability**

19 The data that support the findings of this study are available from corresponding author, CF
20 (clare.fraser@sydney.edu.au), or first author, RS (rob.seymour@ucl.ac.uk). Data can only be shared in a
21 pre-processed and anonymised format, to comply with Macquarie University ethical guidelines.

22 **Results**

23 **Epidemiology**

24 The VSS cohort had a female-to-male ratio of 7/11 with ages ranging from 22 to 45 years old (mean age
25 of 29 ± 7 years). Healthy controls consisted of 5 females and 11 males with ages ranging from 21 to 43
26 years old (mean age of 31 ± 6 years). An independent samples t-test showed that there were no
27 significant differences in age between groups, $t(32)=0.61$, $p=0.546$, $d=0.21$. The average symptom
28 duration was 5 years for the VSS cohort, with 5 patients reporting symptoms since early teenage years.
29 Associated visual and non-visual symptoms are summarised in Table 1. The VSS cohort consisted of
30 100% classic VS with 94% reporting associated palinopsia, 61% photophobia, 72% nyctalopia, and 89%

- 1 other positive visual phenomena. Associated comorbidities included tinnitus in 94%, migraine in 39%,
 2 11% with and 28% without aura, and tremor in 50% of patients.
- 3 In the control group, 12.5% of the cohort reported migraine without aura. No other visual or non-visual
 4 comorbidities were reported.

<i>Visual Symptoms</i>	
Classic Visual Snow	100%
Palinopsias	94%
Photophobia	61%
Nyctalopia	72%
Positive Visual Phenomena	89%
Duration of symptoms >1 year	94%
<i>Non-Visual Symptoms</i>	
Tinnitus	94%
Migraine	39%
Tremor	50%

5 **Table 1:** Visual and non-visual symptoms reported by the VSS cohort.

- 6
- 7 To ensure our results remain significant in regard to the migraine status we conducted a sub-group
 8 analysis for VSS patients with migraine versus those without migraine. The results are reported in
 9 Supplementary Figure 3 – no difference emerged between the sub-groups.

10 **Whole-Brain Alpha and Gamma Power**

- 11 To demonstrate successful source localisation with our LCMV-beamformer pipeline,⁴⁵ see *Materials and*
 12 *Methods*, we calculated changes in gamma power (40-70 Hz) and alpha power (8-13Hz), following
 13 presentation of the visual grating, across an MNI-warped whole-brain 8mm grid. Gamma power (40-
 14 70Hz) and alpha power (8-13Hz) were compared between 0.3-1.5s post-stimulus onset (to capture

1 induced rather than evoked power) and a 1.2s baseline period. As expected, both the control and visual
2 snow participants showed focal increases in gamma power (Figure 2, upper panel) for regions
3 overlapping with primary visual cortex. Both groups also showed decreases in alpha power across the
4 ventral occipital cortex (Figure 2, lower panel), consistent with previous studies.^{49,50}

5 **V1 Gamma Power & Peak Frequency**

6 A time-course from the grid-point showing the maximum change in gamma power within the calcarine
7 sulcus (see *Materials and Methods*) was used for further analysis. An independent t-test was used to
8 investigate group differences in gamma power (averaged across 0.3-1.2s, post-grating onset) and peak
9 frequency. Results showed that gamma power was significantly greater in the VSS group (mean =
10 3.20dB) compared with the control group (mean = 2.27dB), $t(32) = 2.147$, $p = 0.0395$, $d = 0.738$ (also see
11 Figure 3A). This result was not driven by differences in baseline gamma power between groups (see
12 Supplementary Figure 4). There were no significant differences in gamma peak frequency between
13 controls (mean = 52.63Hz) and VSS participants (mean = 53.17Hz), $t(32) = 0.215$, $p = 0.831$, $d = 0.074$
14 (also see Figure 3B).

15 **V1 Alpha Power and Peak Frequency**

16
17 Using the same grid point, we repeated the analysis for the alpha band (8-13Hz), using an independent t-
18 test to compare power and peak frequency between groups. There were no significant differences in alpha
19 power between the VSS group (mean = -1.57dB) compared with the control group (mean = -1.99dB),
20 $t(32) = 0.873$, $p = 0.39$, $d = 0.30$ (also see Figure 3C). There was also no significant difference in alpha
21 peak frequency between groups (control mean = 10.7Hz; VSS mean = 10.8Hz), $t(32) = 0.205$, $p = 0.84$, d
22 $= 0.07$ (also see Figure 3D).

23 **V1 Alpha-Gamma PAC**

24 Using broadband data from V1, changes in alpha-gamma PAC were quantified using an amplitude-
25 corrected mean-vector length algorithm,⁵² which has been shown to be robust for similar MEG data.^{38,54}
26 For the control group, phase-amplitude comodulograms showed increased PAC following presentation
27 of the grating versus baseline, peaking at 8–9Hz phase frequencies and 50–80 Hz amplitude frequencies
28 (Figure 4, left). In contrast, the VSS group displayed lower changes in PAC across the comodulogram,
29 with no clear positive peak (Figure 4, middle). Robust, non-parametric statistics were used to compare
30 groups.⁵¹ For the control>VSS contrast, there was a single positive cluster of greater PAC between 8–9
31 Hz and 54–76 Hz, $p < .05$ two-tailed (Figure 4, right), i.e., coupling between alpha and gamma oscillations
32 during perception in primary visual cortex is reduced in VSS compared to matched controls. We also

1 quantified the effect size of this group difference, using Cohen's d , see Supplementary Figure 5. The
2 maximum value over the comodulogram was $d = 1.24$, which corresponds to a "very large" effect size.

3 **Discussion**

4 By utilising the excellent temporal resolution of magnetoencephalography, alongside beamforming for
5 source localisation, this study supports our initial hypothesis that VSS may be considered a condition of
6 visual dysrhythmia.¹

7 **Alpha-band (8-13Hz) oscillations in VSS**

8 Occipital alpha rhythms dominate recordings made from resting healthy adults,³³ and are involved in the
9 active inhibition of irrelevant visual information.³⁴ Reductions in alpha power measured using EEG/MEG
10 are related to visual attention. Alpha is generally seen as an inhibitory rhythm; however, it is also linked
11 with top-down modulation, prediction, and attentional sampling at $\sim 10\text{Hz}$.^{19,56} In this study, the
12 presentation of a visual grating was accompanied by reductions in occipital alpha-band power,
13 suggesting that participants were attending to the visual grating stimuli. However, there were no group
14 differences in alpha power between VSS and control groups. We also investigated variation in individual
15 alpha peak frequency, as peak alpha frequency is modulated by a variety of factors during perception.⁵⁷
16 However, we found no differences in alpha peak frequency between groups.

17 Relating our findings to tinnitus, a related condition of phantom auditory perception, previous research
18 has reported alterations in alpha-power and resting-state data.^{30,58} However, the literature is very
19 heterogeneous, with both increases and decreases in alpha power being reported.⁵⁹⁻⁶¹ Overall, it seems
20 that neurophysiological mechanisms surrounding a 'release from inhibition' in the visual cortex (via
21 alpha desynchronisation) are not directly involved in disorders of phantom perception. However, this
22 does not rule out atypical mechanisms for top-down control via alpha-band *phase* relationships (see
23 below: *Alpha-Gamma Phase Amplitude Coupling in VSS*).

24 **Gamma-band (40-70Hz) oscillations in VSS**

25 Sensory stimuli elicit increases in high-frequency gamma oscillations generated through excitatory-
26 inhibitory (E-I) neuronal coupling (see Buzsáki & Wang²⁶) Gamma oscillations can be seen as a functional
27 correlate of local neural 'excitability' and facilitate precise and effective inter-regional communication
28 during sensory processing.^{18,27} Recent evidence suggests that gamma oscillations are primarily
29 responsible for the feedforward flow of visual information up the cortical hierarchy.^{62,63}

1 In this study, narrow-band (40-70Hz) oscillations originating from V1 were elicited using a high-contrast
2 visual grating.^{37,50} We found that the VSS group had significantly greater gamma-band power compared
3 to controls. The effect size of this finding was large: 13 out of the 18 VSS patients had gamma power
4 values greater than the mean of the control group. Compared with controls, visual stimuli in VSS
5 patients appear to elicit high-frequency, hyperexcitable activity in early visual cortex. We hypothesise
6 that this hyperexcitable neural activity promotes atypical feedforward flow of information up the
7 cortical hierarchy,^{28,62,63} manifesting as the disorganised white noise or ‘snow’ reported by VSS patients.
8 These novel data highlight the advantages of studying VSS using MEG compared to EEG, where gamma
9 oscillations are harder to measure.^{37,49}

10 Alongside gamma power, we also calculated gamma peak frequency for each participant. Variability in
11 gamma-peak frequency is determined by the balance between excitatory and inhibitory populations of
12 neurons.⁶⁴ However, we found no significant differences in gamma peak frequency between groups.
13 Interestingly, there may be differential neural mechanisms behind the modulation of gamma amplitude
14 versus frequency. Gamma peak frequency seems to be associated with the general “time-constant” of
15 inhibitory processes in E-I circuits (Magazzini et al., 2016), whereas amplitude may be related to the
16 strength of the inhibitory interneuron to superficial pyramidal cell connections.^{65,66}

17 Our results generally complement those findings in a related and frequently co-existing condition:
18 chronic tinnitus, where neuronal hyperexcitability and rapidly enhanced spontaneous firing rates are
19 thought to result in excessive neuronal bursting and synchrony in the auditory cortex.^{67,68} This atypical
20 neural synchrony is particularly linked with spontaneous gamma oscillations, commonly enhanced in
21 tinnitus patients,^{31,59,69} and animal models of tinnitus.⁷⁰ Increased sensory sensitivity, indexed via
22 sensory-specific increases in gamma-band power, is a promising biomarker for disorders of phantom
23 perception.

24 **Alpha-Gamma Phase Amplitude Coupling (PAC) in VSS**

25 Emerging evidence has shown that the power (amplitude) of high-frequency cortical activity in primary
26 sensory areas is modulated via the phase of lower-frequency oscillations.⁷¹ During visual processing, an
27 increase in alpha-gamma phase-amplitude coupling (PAC) is frequently observed in electrophysiological
28 recordings.^{35,36} Alpha-gamma PAC dynamically coordinates brain activity over multiple spatial scales,^{72,73}
29 such that gamma oscillations within local neuronal ensembles are coupled with large-scale patterns of
30 low-frequency phase synchrony.⁷⁴ It is proposed that such dynamics allow information to be routed

1 efficiently between brain areas and for neuronal representations to be segmented and maintained, e.g.,
2 during visual working memory.^{75,76}

3 Following the presentation of a visual grating, we found that in VSS, alpha-gamma PAC in V1 was
4 reduced compared to controls. This reduction occurred despite the VSS group displaying stronger visual
5 gamma power in primary visual cortex. Interestingly, disruptions to PAC have also been reported in
6 tinnitus,⁷⁷ although increased PAC has also been shown.⁷⁸

7 Our findings suggest that visual activity in VSS is both hyperexcitable (increased gamma power) and
8 disorganised (reduced alpha-gamma PAC). Both results could be underpinned by an excitation-inhibition
9 imbalance in visual cortex, as the neurophysiological generation of gamma amplitude and PAC relies
10 heavily on local inhibitory populations of neurons.⁷⁹ Affected local inhibitory processes would produce
11 high-frequency 'noisy' activity and reduced signal-to-noise in perceptual systems, similar to findings
12 reported in tinnitus.^{15,80} However, further corroborating evidence will be required before a definitive link
13 between VSS, E-I interactions, and PAC can be confirmed. Disorganised local activity could also have
14 concomitant effects on establishing inter-regional and global connectivity.⁸¹ Where top-down
15 mechanisms are affected in VSS, altered noise-cancelling (i.e., the "gain") of perceptual systems might
16 result,^{82,83} meaning that typical visual stimuli would produce noisy and hyperactive responses in visual
17 cortex, irrespective of their context.¹ Reduced noise cancelling could explain previous EEG findings of
18 reduced habituation in VSS.¹³ Future studies, specifically targeting perceptual gain and visual feedback
19 pathways,^{28,84} should explore these ideas in more detail.

20 ***Clinical Relevance***

21 From a clinical perspective, our novel findings of increased gamma power and reduced alpha-gamma
22 PAC in VSS suggest that interventions targeting the re-establishment of typical rhythmical activity may
23 help manage and treat the condition. Subject-specific neuromodulation approaches like repetitive TMS
24 and cross-frequency transcranial alternating current stimulation,⁸⁵ or neurofeedback approaches
25 targeting gamma power and/or alpha-gamma PAC could be used for managing VS symptoms.^{86,87}

26 ***Relation to other markers of VSS***

27 Previous research has employed a range of imaging modalities to identify surrogate markers of brain
28 dysfunction in VSS⁸⁸. For example, using ¹⁸F-2-fluoro-2-deoxy-D-glucose PET, Schankin et al⁷ reported
29 hypermetabolism in the lingual gyrus of VSS patients, alongside hypometabolism in the right superior
30 temporal gyrus and the left inferior parietal lobule. Resting-state functional MRI data from a VSS cohort

1 also showed hyperconnectivity between extrastriate and inferior temporal regions and between
2 prefrontal and parietal cortex.¹¹ It is tempting to link hypermetabolism and hyperconnectivity in VSS
3 with our finding of increased gamma-band oscillations. However, the associations between visual
4 gamma, blood oxygen level dependant (BOLD) imaging, and PET are not well established. Generally,
5 increased gamma power is related to increased BOLD⁸⁹, especially for broadband gamma responses⁹⁰.
6 However, the relationship for narrow-band visual gamma is more nuanced (see: Muthukumaraswamy &
7 Singh⁴⁹; Singh⁹¹). It is also important to note that, unlike MEG, both PET and functional MRI data lack the
8 temporal resolution required to measure dynamic changes to neural activity during visual perception.

9 Research utilising structural and functional MRI has reported disruptions to a wide array of brain regions
10 in VSS. For example, increases in grey matter volume are found in lingual gyrus, fusiform gyrus junction,
11 primary and secondary visual cortices, middle and superior temporal gyrus, and parahippocampal
12 gyrus.^{5,7,11} Using functional MRI with a visual paradigm, Puledda and colleagues report decreased BOLD
13 responses in VSS specific for the insula, which were interpreted as disruptions to the salience network.⁵
14 Overall, regions overlapping with extrastriate visual cortex seem to be most commonly associated with
15 VSS.^{5,7,11,88} These regions are responsible for high-level visual processing such as colour vision perception
16 and are linked with palinopsia⁹²: a symptom that was present in 94% of our cohort. Our data extend this
17 work by showing how functional changes in VSS are present even earlier in the visual hierarchy (i.e.,
18 primary visual cortex). These low-level alterations might then propagate downstream to extrastriate
19 regions and beyond.

20 Finally, electrophysiological markers of VSS have reported a number of low-level differences versus
21 controls, including increased N145 latency,¹² and reduced habituation.^{13,93} Our results build on this
22 research by demonstrating differences in the endogenous rhythms of the brain during visual processing.
23 Findings of reduced habituation in VSS are particularly interesting, as they suggest a disrupted noise-
24 cancellation mechanism, which is unable to modulate hyperactive and noisy V1 activity.

25 ***Thalamocortical dysrhythmia***

26 While this study has focussed on dysrhythmias measured from the cortex, it is also essential to consider
27 other brain regions, such as the thalamus. Work over the last few decades suggests that the thalamus
28 does not simply act as a relay station during sensory processing. Instead, there exists a robust network
29 of cortico-thalamic feedback neurons that dynamically influence sensory processing.⁹⁴ One prominent
30 theoretical account termed “thalamocortical dysrhythmia” (TCD) suggests that there is a final common

1 pathway linking disorders of phantom perception, including e.g., migraine, tinnitus, neurogenic pain,
2 and Parkinson's disease,²⁴ that slows the resting state alpha rhythm (8–13Hz) generated by the thalamus
3 to just 4–7 Hz,²⁹ and is accompanied by an increase in gamma power due to changes in lateral inhibition
4 within thalamocortical circuits.^{24,95} We previously proposed this mechanism for VSS (see Lauschke
5 2016¹) and the current paper aims to substantiate this hypothesis. In this cohort of VSS patients, we did
6 not observe any slowing of alpha rhythms measured from the cortex; however, we did observe
7 functionally increased gamma-band power, potentially related to changes in E-I interactions.^{26,73,80}
8 Furthermore, our findings of reduced alpha-gamma PAC in VSS suggest that alpha-rhythms, typically
9 generated by the thalamus, may become decoupled from gamma oscillations in the visual cortex.^{24,36}
10 Interestingly, under the TCD framework,²⁴ if thalamic rhythms have slowed to 4-7Hz in VSS, the visual
11 cortex may become preferentially entrained to the theta rhythm (i.e., increased theta-gamma PAC).
12 However, in this study, the length of each trial was insufficient to accurately quantify theta-gamma
13 coupling.³⁸

14 To further test the TCD framework, future work should focus on studying potential dysthymias directly
15 within the thalamus and/or via thalamocortical connectivity. While, deep-brain structures like the
16 thalamus are notoriously challenging to measure with non-invasive arrays of MEG sensors placed
17 outside the head,²⁰ recent progress has shown that it is possible,⁹⁶ given certain constraints.^{97,98}
18 However, in this study, the quality of the MEG-MRI co-registration, and the resulting forward model,
19 were not good enough for reliably measuring subcortical activity. Therefore, future work should aim to
20 utilise *subject-specific* 3D-printed scanner-casts and high-quality structural MRI scans in VSS cohorts.

21 **Limitations**

22 Our study is based on a relatively small number of VSS and control participants. Participant recruitment
23 was cut short by the COVID-19 pandemic. However, the effect sizes of group differences should be
24 considered: $d = 0.738$ for gamma power (which can be described as “medium” to “large”); and $d = 1.24$
25 for the alpha-gamma PAC result (which can be described as “very large”). In terms of participant
26 demographics, it should be noted that we were unable to control for migraine symptomology between
27 groups: 39% for the visual snow cohort reported migraine; versus 6.2% for the control group. Given that
28 perceptual disturbances similar to visual snow are commonly reported by some migraine patients,^{2,3} we
29 ran an exploratory sub-group analysis, to determine whether our results were driven by concurrent
30 presence of migraine in the VSS group (see Supplementary Figure 5). No clear patterns emerged to
31 suggest a distinction between groups based on the presence or not of migraine. The extant literature

1 regarding gamma power in migraine is heterogenous. For example, Hall and colleagues⁹⁹ reported
2 gamma-band desynchronisation (lower power) during visual aura, preceding headache. However, one
3 recent study¹⁰⁰ reported increased gamma-power in migraine patients versus controls, but for evoked¹⁰¹
4 rather than induced gamma. This strengthens our confidence that the group results reported in this
5 manuscript are related to visual snow symptomology rather than migraine. Future studies should
6 replicate and extend our findings with larger cohorts of visual snow patients, migraine patients and
7 healthy controls. This would allow a detailed statistical comparison of oscillatory power and PAC in
8 migraine versus visual snow. Larger cohorts of participants would also allow neuroimaging findings to be
9 directly related to the clinical symptoms of the condition, a crucial consideration given that VSS exists on
10 a continuum with significant variances in the severity of reported symptoms.^{1,9} Finally, this study opted
11 to use a high-contrast visual grating to elicit specific visual oscillations in the early visual cortex.
12 However, it remains unclear whether our findings generalise to more complex perceptual stimuli.
13 Interestingly, VSS patients report that certain stimuli trigger “snow” symptoms more than others. More
14 naturalistic stimuli (e.g., images and videos) combined with MEG could be used to isolate which
15 particular aspects of the visual world intensify VSS symptoms. Immersive virtual reality environments
16 could also be used in combination with new wearable MEG systems.¹⁰²

17 **Conclusion**

18 This study used MEG to study neuronal oscillations during visual processing in a cohort of visual snow
19 syndrome (VSS) patients and control participants. Compared with controls, VSS patients displayed
20 significantly increased gamma (40-70Hz) power in the primary visual cortex and reduced phase-
21 amplitude coupling, suggesting that cortical activity in VSS during early visual processing is hyperactive
22 and disorganised, results that are consistent with theories of thalamocortical dysrhythmia.

23 **Acknowledgements**

24 We wish to thank all the patients and volunteers who gave their time to participate in this research
25 study. We also acknowledge Nick Benikos and Stan Tarnavskii for MEG technical assistance.

26 **Funding**

27 The research was supported by the 2018 North American Neuro-Ophthalmology Society Pilot Grant for
28 research into Visual Snow.

1 Competing interests

2 The authors have no conflict of interest or financial disclosures

3 Supplementary material

4 This manuscript is accompanied by supplementary material.

5 References:

- 6 1. Lauschke JL, Plant GT, Fraser CL. Visual snow: a thalamocortical dysrhythmia of the
7 visual pathway? *J Clin Neurosci.* 2016;28:123-127.
- 8 2. Liu GT, Schatz NJ, Galetta SL, Volpe NJ, Skobieranda F, Kosmorsky GS. Persistent
9 positive visual phenomena in migraine. *Neurology.* 1995;45(4):664-668.
- 10 3. Schankin CJ, Maniyar FH, Digre KB, Goadsby PJ. ‘Visual snow’—a disorder distinct from
11 persistent migraine aura. *Brain.* 2014;137(5):1419-1428.
- 12 4. Sastre-Ibanez M, Santos-Bueso E, Porta-Etessam J, García-Feijoo J. Visual snow: report of
13 three cases. *J Fr Ophthalmol.* 2015;38(7):e157-e158.
- 14 5. Puledra F, Ffytche D, Lythgoe DJ, et al. Insular and occipital changes in visual snow
15 syndrome: a BOLD fMRI and MRS study. *Ann Clin Transl Neurol.* 2020;7(3):296-306.
16 doi:https://doi.org/10.1002/acn3.50986
- 17 6. White OB, Clough M, McKendrick AM, Fielding J. Visual snow: visual misperception. *J*
18 *Neuroophthalmol.* 2018;38(4):514-521.
- 19 7. Schankin CJ, Maniyar FH, Chou DE, Eller M, Sprenger T, Goadsby PJ. Structural and
20 functional footprint of visual snow syndrome. *Brain.* 2020;143(4):1106-1113.
- 21 8. Kondziella D, Olsen MH, Dreier JP. Prevalence of visual snow syndrome in the UK. *Eur J*
22 *Neurol.* 2020;27(5):764-772. doi:https://doi.org/10.1111/ene.14150
- 23 9. Wood H. Shedding new light on visual snow syndrome. *Nat Rev Neurol.* 2020;16(4):183-
24 183. doi:10.1038/s41582-020-0324-8
- 25 10. Shibata M, Tsutsumi K, Iwabuchi Y, et al. [123I]-IMP single-photon emission computed
26 tomography imaging in visual snow syndrome: A case series. *Cephalalgia.*
27 2020;40(14):1671-1675.
- 28 11. Aldusary N, Traber GL, Freund P, et al. Abnormal connectivity and brain structure in
29 patients with visual snow. *Front Hum Neurosci.* 2020;14:476.

- 1 12. Eren O, Rauschel V, Ruscheweyh R, Straube A, Schankin CJ. Evidence of dysfunction in
2 the visual association cortex in visual snow syndrome. *Ann Neurol.* 2018;84(6):946-949.
3 doi:<https://doi.org/10.1002/ana.25372>
- 4 13. Luna S, Lai D, Harris A. Antagonistic Relationship Between VEP Potentiation and Gamma
5 Power in Visual Snow Syndrome. *Headache J Head Face Pain.* 2018;58(1):138-144.
6 doi:<https://doi.org/10.1111/head.13231>
- 7 14. Polack P-O, Friedman J, Golshani P. Cellular mechanisms of brain state-dependent gain
8 modulation in visual cortex. *Nat Neurosci.* 2013;16(9):1331-1339. doi:10.1038/nn.3464
- 9 15. Rauschecker JP, Leaver AM, Mühlau M. Tuning Out the Noise: Limbic-Auditory
10 Interactions in Tinnitus. *Neuron.* 2010;66(6):819-826. doi:10.1016/j.neuron.2010.04.032
- 11 16. Bou Ghannam A, Pelak VS. Visual Snow: a Potential Cortical Hyperexcitability Syndrome.
12 *Curr Treat Options Neurol.* 2017;19(3):9. doi:10.1007/s11940-017-0448-3
- 13 17. Arnal LH, Giraud A-L. Cortical oscillations and sensory predictions. *Trends Cogn Sci.*
14 2012;16(7):390-398.
- 15 18. Bastos AM, Vezoli J, Fries P. Communication through coherence with inter-areal delays.
16 *Curr Opin Neurobiol.* 2015;31:173-180.
- 17 19. Clayton MS, Yeung N, Cohen Kadosh R. The many characters of visual alpha oscillations.
18 *Eur J Neurosci.* 2018;48(7):2498-2508.
- 19 20. Baillet S. Magnetoencephalography for brain electrophysiology and imaging. *Nat Neurosci.*
20 2017;20(3):327-339.
- 21 21. Hendry SH, Reid RC. The koniocellular pathway in primate vision. *Annu Rev Neurosci.*
22 2000;23(1):127-153.
- 23 22. Cheong SK, Tailby C, Martin PR, Levitt JB, Solomon SG. Slow intrinsic rhythm in the
24 koniocellular visual pathway. *Proc Natl Acad Sci.* 2011;108(35):14659-14663.
- 25 23. De Tommaso M, Ambrosini A, Brighina F, et al. Altered processing of sensory stimuli in
26 patients with migraine. *Nat Rev Neurol.* 2014;10(3):144.
- 27 24. De Ridder D, Vanneste S, Langguth B, Llinas R. Thalamocortical Dysrhythmia: A
28 Theoretical Update in Tinnitus. *Front Neurol.* 2015;6. doi:10.3389/fneur.2015.00124
- 29 25. Ferrari MD, Klever RR, Terwindt GM, Ayata C, van den Maagdenberg AM. Migraine
30 pathophysiology: lessons from mouse models and human genetics. *Lancet Neurol.*
31 2015;14(1):65-80.
- 32 26. Buzsáki G, Wang X-J. Mechanisms of gamma oscillations. *Annu Rev Neurosci.*
33 2012;35:203.

- 1 27. Fries P. Rhythms for cognition: communication through coherence. *Neuron*.
2 2015;88(1):220-235.
- 3 28. Michalareas G, Vezoli J, Van Pelt S, Schoffelen J-M, Kennedy H, Fries P. Alpha-beta and
4 gamma rhythms subserve feedback and feedforward influences among human visual
5 cortical areas. *Neuron*. 2016;89(2):384-397.
- 6 29. Llinás RR, Ribary U, Jeanmonod D, Kronberg E, Mitra PP. Thalamocortical dysrhythmia: a
7 neurological and neuropsychiatric syndrome characterized by magnetoencephalography.
8 *Proc Natl Acad Sci*. 1999;96(26):15222-15227.
- 9 30. Weisz N, Moratti S, Meinzer M, Dohrmann K, Elbert T. Tinnitus Perception and Distress Is
10 Related to Abnormal Spontaneous Brain Activity as Measured by
11 Magnetoencephalography. *PLOS Med*. 2005;2(6):e153. doi:10.1371/journal.pmed.0020153
- 12 31. Weisz N, Müller S, Schlee W, Dohrmann K, Hartmann T, Elbert T. The neural code of
13 auditory phantom perception. *J Neurosci*. 2007;27(6):1479-1484.
- 14 32. Schulman JJ, Cancro R, Lowe III S, Lu F, Walton KD, Llinás RR. Imaging of
15 thalamocortical dysrhythmia in neuropsychiatry. *Front Hum Neurosci*. 2011;5:69.
- 16 33. Klimesch W. Alpha-band oscillations, attention, and controlled access to stored
17 information. *Trends Cogn Sci*. 2012;16(12):606-617. doi:10.1016/j.tics.2012.10.007
- 18 34. Jensen O, Mazaheri A. Shaping functional architecture by oscillatory alpha activity: gating
19 by inhibition. *Front Hum Neurosci*. 2010;4:186.
- 20 35. Voytek B, Canolty RT, Shestiyuk A, Crone N, Parvizi J, Knight RT. Shifts in Gamma
21 Phase–Amplitude Coupling Frequency from Theta to Alpha Over Posterior Cortex During
22 Visual Tasks. *Front Hum Neurosci*. 2010;4. doi:10.3389/fnhum.2010.00191
- 23 36. Spaak E, Bonnefond M, Maier A, Leopold DA, Jensen O. Layer-specific entrainment of
24 gamma-band neural activity by the alpha rhythm in monkey visual cortex. *Curr Biol*.
25 2012;22(24):2313-2318.
- 26 37. Muthukumaraswamy SD. High-frequency brain activity and muscle artifacts in MEG/EEG:
27 a review and recommendations. *Front Hum Neurosci*. 2013;7.
28 doi:10.3389/fnhum.2013.00138
- 29 38. Seymour RA, Rippon G, Kessler K. The Detection of Phase Amplitude Coupling during
30 Sensory Processing. *Front Neurosci*. 2017;11:487.
- 31 39. Taulu S, Simola J. Spatiotemporal signal space separation method for rejecting nearby
32 interference in MEG measurements. *Phys Med Biol*. 2006;51(7):1759.
- 33 40. Oostenveld R, Fries P, Maris E, Schoffelen J-M. FieldTrip: open source software for
34 advanced analysis of MEG, EEG, and invasive electrophysiological data. *Comput Intell*
35 *Neurosci*. 2011;2011:1.

- 1 41. Larson-Prior LJ, Oostenveld R, Della Penna S, et al. Adding dynamics to the Human
2 Connectome Project with MEG. *Neuroimage*. 2013;80:190-201.
- 3 42. Gohel B, Lim S, Kim M-Y, Kwon H, Kim K. Approximate Subject Specific Pseudo MRI
4 from an Available MRI Dataset for MEG Source Imaging. *Front Neuroinformatics*.
5 2017;11:50.
- 6 43. Seymour R. *Macquarie-MEG-Research/MEMES: For Zenodo.*; 2018.
7 doi:10.5281/zenodo.1451031
- 8 44. Nolte G. The magnetic lead field theorem in the quasi-static approximation and its use for
9 magnetoencephalography forward calculation in realistic volume conductors. *Phys Med
10 Biol*. 2003;48(22):3637-3652.
- 11 45. Van Veen BD, van Drongelen W, Yuchtman M, Suzuki A. Localization of brain electrical
12 activity via linearly constrained minimum variance spatial filtering. *IEEE Trans Biomed
13 Eng*. 1997;44(9):867-880. doi:10.1109/10.623056
- 14 46. Brookes MJ, Vrba J, Robinson SE, et al. Optimising experimental design for MEG
15 beamformer imaging. *Neuroimage*. 2008;39(4):1788-1802.
- 16 47. Tzourio-Mazoyer N, Landeau B, Papathanassiou D, et al. Automated anatomical labeling of
17 activations in SPM using a macroscopic anatomical parcellation of the MNI MRI single-
18 subject brain. *Neuroimage*. 2002;15(1):273-289.
- 19 48. Bruns A, Eckhorn R. Task-related coupling from high- to low-frequency signals among
20 visual cortical areas in human subdural recordings. *Int J Psychophysiol*. 2004;51(2):97-116.
21 doi:10.1016/j.ijpsycho.2003.07.001
- 22 49. Muthukumaraswamy SD, Singh KD. Spatiotemporal frequency tuning of BOLD and
23 gamma band MEG responses compared in primary visual cortex. *NeuroImage*.
24 2008;40(4):1552-1560. doi:10.1016/j.neuroimage.2008.01.052
- 25 50. Hoogenboom N, Schoffelen J-M, Oostenveld R, Parkes LM, Fries P. Localizing human
26 visual gamma-band activity in frequency, time and space. *Neuroimage*. 2006;29(3):764-
27 773.
- 28 51. Maris E, Oostenveld R. Nonparametric statistical testing of EEG- and MEG-data. *J
29 Neurosci Methods*. 2007;164(1):177-190. doi:10.1016/j.jneumeth.2007.03.024
- 30 52. Özkurt TE, Schnitzler A. A critical note on the definition of phase–amplitude cross-
31 frequency coupling. *J Neurosci Methods*. 2011;201(2):438-443.
- 32 53. Love J, Selker R, Marsman M, et al. JASP: Graphical statistical software for common
33 statistical designs. *J Stat Softw*. 2019;88(2):1-17.

- 1 54. Seymour RA, Rippon G, Gooding-Williams G, Schoffelen JM, Kessler K. Dysregulated
2 oscillatory connectivity in the visual system in autism spectrum disorder. *Brain*.
3 2019;142(10):3294-3305. doi:10.1093/brain/awz214
- 4 55. Klimesch W. EEG alpha and theta oscillations reflect cognitive and memory performance: a
5 review and analysis. *Brain Res Rev*. 1999;29(2):169-195.
- 6 56. Sokoliuk R, VanRullen R. The flickering wheel illusion: When α rhythms make a static
7 wheel flicker. *J Neurosci*. 2013;33(33):13498-13504.
- 8 57. Haegens S, Cousijn H, Wallis G, Harrison PJ, Nobre AC. Inter- and intra-individual
9 variability in alpha peak frequency. *NeuroImage*. 2014;92:46-55.
10 doi:10.1016/j.neuroimage.2014.01.049
- 11 58. Schlee W, Schecklmann M, Lehner A, et al. Reduced variability of auditory alpha activity
12 in chronic tinnitus. *Neural Plast*. 2014;2014.
- 13 59. Lorenz I, Müller N, Schlee W, Hartmann T, Weisz N. Loss of alpha power is related to
14 increased gamma synchronization—A marker of reduced inhibition in tinnitus? *Neurosci*
15 *Lett*. 2009;453(3):225-228. doi:10.1016/j.neulet.2009.02.028
- 16 60. Moazami-Goudarzi M, Michels L, Weisz N, Jeanmonod D. Temporo-insular enhancement
17 of EEG low and high frequencies in patients with chronic tinnitus. QEEG study of chronic
18 tinnitus patients. *BMC Neurosci*. 2010;11(1):1-12.
- 19 61. Sedley W, Gander PE, Kumar S, et al. Intracranial mapping of a cortical tinnitus system
20 using residual inhibition. *Curr Biol*. 2015;25(9):1208-1214.
- 21 62. Bastos, Vezoli J, Bosman CA, et al. Visual Areas Exert Feedforward and Feedback
22 Influences through Distinct Frequency Channels. *Neuron*. 2015;85(2):390-401.
23 doi:10.1016/j.neuron.2014.12.018
- 24 63. Jensen O, Bonnefond M, Marshall TR, Tiesinga P. Oscillatory mechanisms of feedforward
25 and feedback visual processing. *Trends Neurosci*. 2015;38(4):192-194.
- 26 64. Brunel N, Wang X-J. What determines the frequency of fast network oscillations with
27 irregular neural discharges? I. Synaptic dynamics and excitation-inhibition balance. *J*
28 *Neurophysiol*. 2003;90(1):415-430.
- 29 65. Shaw AD, Moran RJ, Muthukumaraswamy SD, et al. Neurophysiologically-informed
30 markers of individual variability and pharmacological manipulation of human cortical
31 gamma. *Neuroimage*. 2017;161:19-31.
- 32 66. Sumner RL, McMillan RL, Shaw AD, Singh KD, Sundram F, Muthukumaraswamy SD.
33 Peak visual gamma frequency is modified across the healthy menstrual cycle. *Hum Brain*
34 *Mapp*. 2018;39(8):3187-3202. doi:https://doi.org/10.1002/hbm.24069

- 1 67. Noreña AJ, Farley BJ. Tinnitus-related neural activity: theories of generation, propagation,
2 and centralization. *Hear Res.* 2013;295:161-171.
- 3 68. Eggermont JJ, Tass PA. Maladaptive neural synchrony in tinnitus: origin and restoration.
4 *Front Neurol.* 2015;6:29.
- 5 69. Vanneste S, To WT, De Ridder D. Tinnitus and neuropathic pain share a common neural
6 substrate in the form of specific brain connectivity and microstate profiles. *Prog*
7 *Neuropsychopharmacol Biol Psychiatry.* 2019;88:388-400.
- 8 70. Tziridis K, Ahlf S, Jeschke M, Happel MF, Ohl FW, Schulze H. Noise trauma induced
9 neural plasticity throughout the auditory system of Mongolian gerbils: differences between
10 tinnitus developing and non-developing animals. *Front Neurol.* 2015;6:22.
- 11 71. Canolty RT, Edwards E, Dalal SS, et al. High gamma power is phase-locked to theta
12 oscillations in human neocortex. *science.* 2006;313(5793):1626-1628.
- 13 72. Florin E, Baillet S. The brain's resting-state activity is shaped by synchronized cross-
14 frequency coupling of neural oscillations. *NeuroImage.* 2015;111:26-35.
15 doi:10.1016/j.neuroimage.2015.01.054
- 16 73. Kessler K, Seymour RA, Rippon G. Brain oscillations and connectivity in autism spectrum
17 disorders (ASD): new approaches to methodology, measurement and modelling. *Neurosci*
18 *Biobehav Rev.* 2016;71:601-620. doi:10.1016/j.neubiorev.2016.10.002
- 19 74. Bonnefond M, Kastner S, Jensen O. Communication between Brain Areas Based on Nested
20 Oscillations. *ENeuro.* 2017;4(2):ENEURO-0153.
- 21 75. Lisman JE, Idiart MA. Storage of 7 plus/minus 2 short-term memories in oscillatory
22 subcycles. *Science.* 1995;267(5203):1512.
- 23 76. Bonnefond M, Jensen O. Gamma Activity Coupled to Alpha Phase as a Mechanism for
24 Top-Down Controlled Gating. *PLOS ONE.* 2015;10(6):e0128667.
25 doi:10.1371/journal.pone.0128667
- 26 77. Ahn M-H, Hong SK, Min B-K. The absence of resting-state high-gamma cross-frequency
27 coupling in patients with tinnitus. *Hear Res.* 2017;356:63-73.
- 28 78. Adamchic I, Langguth B, Hauptmann C, Tass PA. Abnormal cross-frequency coupling in
29 the tinnitus network. *Front Neurosci.* 2014;8. doi:10.3389/fnins.2014.00284
- 30 79. Onslow ACE, Jones MW, Bogacz R. A canonical circuit for generating phase-amplitude
31 coupling. *PloS One.* 2014;9(8):e102591. doi:10.1371/journal.pone.0102591
- 32 80. Rubenstein JLR, Merzenich MM. Model of autism: increased ratio of excitation/inhibition
33 in key neural systems. *Genes Brain Behav.* 2003;2(5):255-267.

- 1 81. Voytek B, Knight RT. Dynamic network communication as a unifying neural basis for
2 cognition, development, aging, and disease. *Biol Psychiatry*. 2015;77(12):1089-1097.
- 3 82. Tiesinga PH, Fellous J-M, Salinas E, José JV, Sejnowski TJ. Inhibitory synchrony as a
4 mechanism for attentional gain modulation. *J Physiol-Paris*. 2004;98(4):296-314.
- 5 83. Sedley W, Friston KJ, Gander PE, Kumar S, Griffiths TD. An integrative tinnitus model
6 based on sensory precision. *Trends Neurosci*. 2016;39(12):799-812.
- 7 84. Flounders MW, González-García C, Hardstone R, He BJ. Neural dynamics of visual
8 ambiguity resolution by perceptual prior. *eLife*. 2019;8:e41861.
- 9 85. Riddle J, McFerren A, Frohlich F. Causal role of cross-frequency coupling in distinct
10 components of cognitive control. *Prog Neurobiol*. Published online March 16,
11 2021:102033. doi:10.1016/j.pneurobio.2021.102033
- 12 86. Salari N, Büchel C, Rose M. Neurofeedback training of gamma band oscillations improves
13 perceptual processing. *Exp Brain Res*. 2014;232(10):3353-3361.
- 14 87. Chauvière L, Singer W. Neurofeedback training of gamma oscillations in monkey primary
15 visual cortex. *Cereb Cortex*. 2019;29(11):4785-4802.
- 16 88. Traber GL, Aldusary N, Freund P, et al. Visual snow patients show functional
17 hyperconnectivity and structural abnormalities of brain regions involved in visual
18 processing. *Invest Ophthalmol Vis Sci*. 2020;61(7):3387-3387.
- 19 89. Logothetis NK, Pauls J, Augath M, Trinath T, Oeltermann A. Neurophysiological
20 investigation of the basis of the fMRI signal. *Nature*. 2001;412(6843):150-157.
21 doi:10.1038/35084005
- 22 90. Winawer J, Kay KN, Foster BL, Rauschecker AM, Parvizi J, Wandell BA. Asynchronous
23 Broadband Signals Are the Principal Source of the BOLD Response in Human Visual
24 Cortex. *Curr Biol*. 2013;23(13):1145-1153. doi:10.1016/j.cub.2013.05.001
- 25 91. Singh KD. Which “neural activity” do you mean? fMRI, MEG, oscillations and
26 neurotransmitters. *Neuroimage*. 2012;62(2):1121-1130.
- 27 92. Gersztenkorn D, Lee AG. Palinopsia revamped: a systematic review of the literature. *Surv*
28 *Ophthalmol*. 2015;60(1):1-35.
- 29 93. Yildiz FG, Turkyilmaz U, Unal- Cevik I. The Clinical Characteristics and
30 Neurophysiological Assessments of the Occipital Cortex in Visual Snow Syndrome With or
31 Without Migraine. *Headache J Head Face Pain*. 2019;59(4):484-494.
32 doi:https://doi.org/10.1111/head.13494
- 33 94. Briggs F, Usrey WM. Emerging views of corticothalamic function. *Curr Opin Neurobiol*.
34 2008;18(4):403-407.

- 1 95. Llinás R, Urbano FJ, Leznik E, Ramírez RR, Van Marle HJ. Rhythmic and dysrhythmic
2 thalamocortical dynamics: GABA systems and the edge effect. *Trends Neurosci.*
3 2005;28(6):325-333.
- 4 96. Pu Y, Cheyne DO, Cornwell BR, Johnson BW. Non-invasive investigation of human
5 hippocampal rhythms using magnetoencephalography: a review. *Front Neurosci.*
6 2018;12:273.
- 7 97. Meyer SS, Rossiter H, Brookes MJ, Woolrich MW, Bestmann S, Barnes GR. Using
8 generative models to make probabilistic statements about hippocampal engagement in
9 MEG. *Neuroimage.* 2017;149:468-482.
- 10 98. Tierney TM, Levy A, Barry DN, et al. Mouth magnetoencephalography: A unique
11 perspective on the human hippocampus. *NeuroImage.* 2021;225:117443.
- 12 99. Hall SD, Barnes GR, Hillebrand A, Furlong PL, Singh KD, Holliday IE. Spatio-temporal
13 Imaging of Cortical Desynchronization in Migraine Visual Aura: A
14 Magnetoencephalography Case Study. *Headache J Head Face Pain.* 2004;44(3):204-208.
15 doi:10.1111/j.1526-4610.2004.04048.x
- 16 100. Lisicki M, D'Ostilio K, Coppola G, et al. Headache Related Alterations of Visual
17 Processing in Migraine Patients. *J Pain.* 2020;21(5):593-602.
18 doi:10.1016/j.jpain.2019.08.017
- 19 101. Seymour RA, Rippon G, Gooding-Williams G, Sowman PF, Kessler K. Reduced auditory
20 steady state responses in autism spectrum disorder. *Mol Autism.* 2020;11(1):1-13.
- 21 102. Roberts G, Holmes N, Alexander N, et al. Towards OPM-MEG in a virtual reality
22 environment. *NeuroImage.* 2019;199:408-417. doi:10.1016/j.neuroimage.2019.06.010

1 **Figure legends**

2 **Figure 1:**

3 **Experimental paradigm.** Following a 2.0s, 3.0s, or 4.0s baseline period, participants were presented
4 with a visual grating (1.5s duration). A cartoon alien or astronaut picture (duration 1.0s) was then
5 presented. The subsequent presentation of a '?' symbol was the imperative signal for a response to an
6 alien (response time up to 1.0 s). Participants were instructed to provide no response to astronauts. The
7 alien/astronaut stimuli were to maintain attention and were not part of the analysed data.

8 **Figure 2:**

9 **Whole brain representation** Following visual grating presentation, the change (dB) in gamma power
10 (40-70Hz; 0.3-1.5s, upper panel) and alpha power (8-13Hz, 0.3-1.5s, lower panel) were calculated across
11 a whole-brain grid. Results for the control group (left) and VSS group (right) were averaged and
12 interpolated onto a 3D cortical mesh and finally thresholded at values greater than 1.3dB (gamma) and
13 less than -0.3dB (alpha) for illustrative purposes.

14 **Figure 3:**

15 **V1 Power and Peak Frequency.** For both control and VSS groups, violin plots were produced (with
16 median and interquartile range lines) to show: (A) V1 gamma power; (B) V1 peak frequency; (C) V1
17 alpha power; (D) V1 alpha peak frequency. Dots correspond to data from individual participants. Group
18 differences were analysed using an independent samples t-test, two-tailed.

19 **Figure 4:**

20 **V1 phase-amplitude coupling.** The control group showed increased alpha-gamma PAC compared with
21 baseline, with a peak between 50–80 Hz amplitude and 8–9 Hz phase. The VSS group showed less
22 prominent increases in PAC across the comodulogram. Non-parametric statistical comparison (see
23 'Methods') indicated significantly greater PAC for the control compared to the VSS group ($p < .05$) from
24 54–76 Hz amplitude and 8–9 Hz phase.

25

26

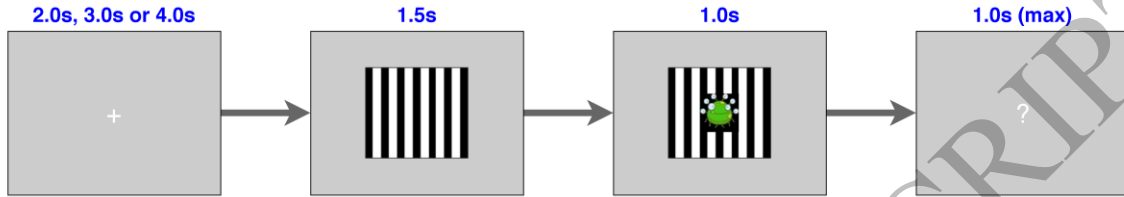


Figure 1
159x110 mm (6.2 x DPI)

1
2
3
4

ACCEPTED MANUSCRIPT

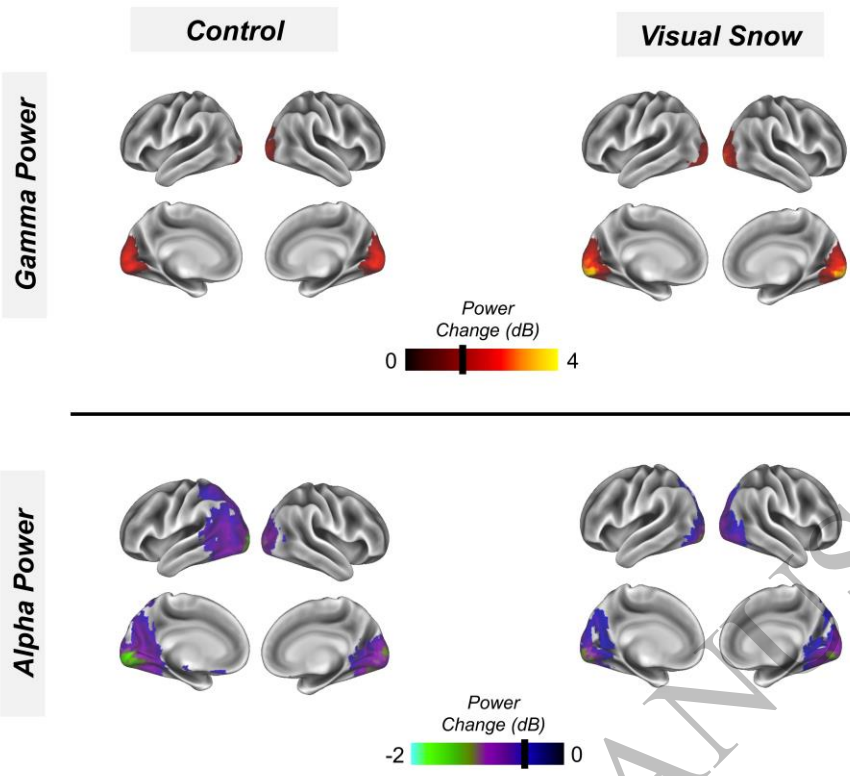


Figure 2
159x110 mm (6.2 x DPI)

1
2
3
4

ACCEPTED MANUSCRIPT

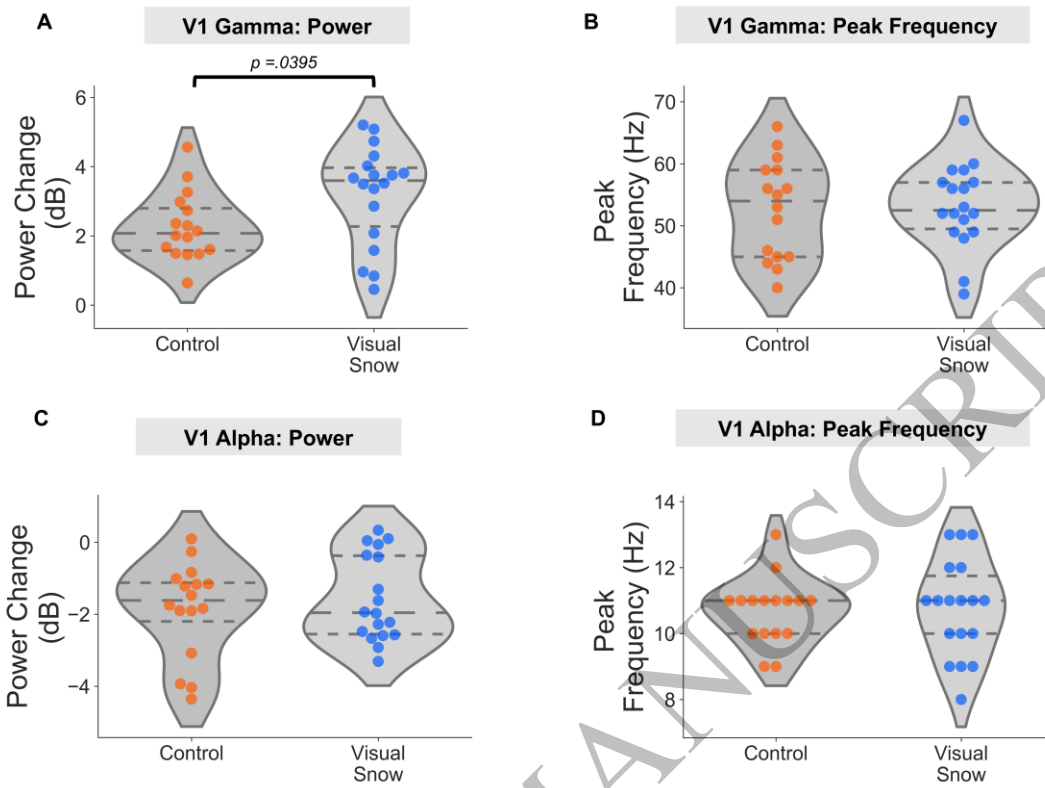


Figure 3
 159x113 mm (6.2 x DPI)

1
 2
 3
 4

V1 Phase Amplitude Coupling

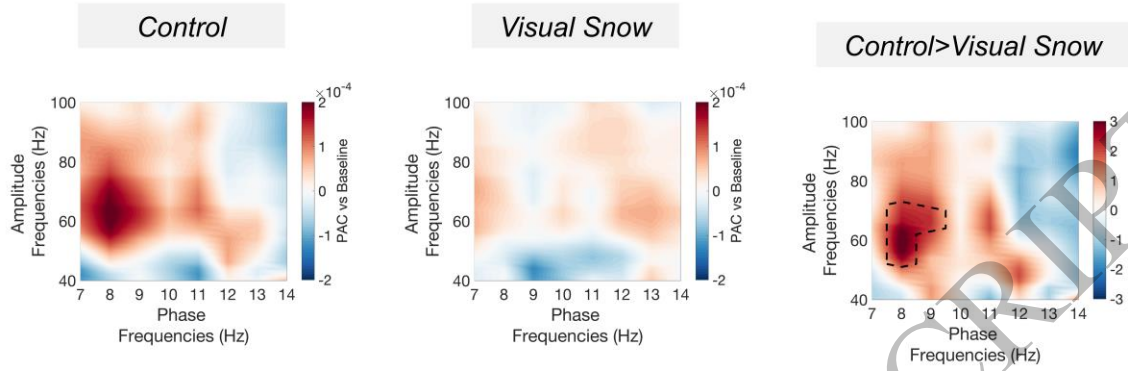


Figure 4
159x110 mm (6.2 x DPI)

1
2
3
4

1 **Abbreviated summary**

2 Hepschke/Seymour et al report that rhythmical brain activity in the visual cortex of patients with visual
3 snow syndrome is hyperexcitable and disorganised compared to control patients, when examined using
4 magnetoencephalographic techniques. This provides evidence that visual snow syndrome may a
5 disorder of (thalamo-) cortical dysrhythmias.

ACCEPTED MANUSCRIPT